

Structure-Dependent Electrical, Optical and Magnetic Properties of Mn-Doped BiFeO₃ Thin Films Prepared by the Sol-Gel Process

Jin Li¹, Kaitong Liu⁴, Jinbao Xu¹, Lei Wang^{2,3}, Liang Bian¹ & Fanglong Xu^{2,3}

¹Key Laboratory of Functional Materials and Devices for Special Environments, Chinese Academy of Sciences, Urumqi, Xinjiang, China

²Xinjiang Key Laboratory of Electronic Information Materials and Devices, Urumqi, Xinjiang, China

³University of Chinese Academy of Sciences, Beijing, China

⁴Department of Physics, XinJiang University, Urumqi, Xinjiang, China

Correspondence: Jinbao Xu, Xinjiang Key Laboratory of Electronic Information Materials and Devices, Xinjiang Technical Institute of Physics & Chemistry, Chinese Academy of Sciences, Urumqi 830011, China. Tel: 86-991-383-5096. E-mail: xujb@ms.xjb.ac.cn

Received: April 15, 2013 Accepted: May 23, 2013 Online Published: May 28, 2013

doi:10.5539/jmsr.v2n3p75

URL: <http://dx.doi.org/10.5539/jmsr.v2n3p75>

Abstract

The effect of Mn doping on crystal structure, electric, magnetic and optical properties of BiFeO₃ thin films prepared via the sol-gel process on indium tin oxide/glass substrates was studied. X-ray diffraction analysis indicated that Mn-doped BiFeO₃ thin films presented single tetragonal structure with P4mm symmetry. Compared with the pure BiFeO₃ film, the resistivity was found to increase while leakage current density and optical band gap decreased in low Mn content ($\leq 7.5\%$) doped BiFeO₃ system. An evident magnetic hysteresis loop was observed for all the thin films at room temperature and Mn-doped BiFeO₃ films showed a larger saturated magnetization than pure BiFeO₃ film.

Keywords: films, electrical conductivity, magnetic property, optical property

1. Introduction

Magnetoelectric multiferroics, such as BiFeO₃ (BFO), simultaneously exhibit ferroelectricity and ferromagnetism orders. Such materials continue to attract great fundamental scientific interests in past several years due to their potential application in multifunctional devices, such as the data storage, magnetic filter, and sensors (Kumar et al., 2000; Maccheshn et al., 1966; Neaton et al., 2005).

In recent years, BFO thin films have drawn people more and more attention because of its more excellent physical properties than BFO bulk, such as spontaneous polarization (Wang et al., 2003), saturation magnetization (Yun et al., 2004), and a piezoelectric response (Zeches et al., 2009).

However, low-resistivity of BFO thin films still is a major problem for its potential application in various micro-electromechanical system devices. The mechanism inducing resistivity in BFO films can be attributed to the variable oxidation states of Fe ions (Fe³⁺ to Fe²⁺), which requires oxygen vacancies (V_O²⁺) for charge compensation and produces electron hopping in films (Yun et al., 2003; Wu et al., 2011). Another mechanism is due to high volatility of atom Bi which generates V_{Bi}³⁺ vacancies in lattice accompanied by the emergence of the second-phase (such as Bi₂Fe₄O₉) (Uchida et al., 2006). The V_O²⁺ and V_{Bi}³⁺ vacancies are highly mobile and inclined to reduce resistivity on the application of electric field. In order to solve the low-resistivity problem, solid solution of BFO with another ABO₃ materials, such as BaTiO₃ (Kumar et al., 2000), has been used to inhibit the volatility of Bi atom which can increase sample resistivity. In addition, the site-engineering concept in Bi-site or Fe-site has been proposed to control volatility of Bi atom and suppress generation of oxygen vacancies (Zhang et al., 2010; Wei et al., 2010). However, in the case of the sol-gel process, it can be found that BFO thin films were always obtained at around 550 °C which is lower than the volatility temperature of Bi atom (~700 °C). For this reason, we thought the variable valences of Fe atom should play more important role in inducing resistivity of BFO thin films, rather than volatility of atom Bi.

In this paper, we attempt to further improve the resistivity of BFO thin films by Mn²⁺ doping. Mn-doped BFO

thin films were prepared on indium tin oxide (ITO)/Glass substrate. ITO layer is semiconductor-like transparent thin film which can be used to as electrode to investigate the optical property of the thin films. The structural phase transition, resistivity, optical and magnetic properties of Mn-doped BFO thin films were discussed in detail.

2. Experimental Procedures

Pure BiFeO₃ and Mn-doped BiFeO₃ (Mn/Fe=0.0at. %, 2.5at. %, 5.0at. %, 7.5at. % and 10 at.%) thin films were prepared on ITO/Glass substrates by a conventional sol-gel process. The bismuth nitrate Bi(NO₃)₃·5H₂O, iron nitrate Fe(NO₃)₃·9H₂O and manganese acetate(C₄H₆MnO₄·4H₂O) were mixed in citric acid under constant stirring at 80 °C for 30min and then 2-methoxyethanol was added under constant stirring for 180min at room temperature. The depositions were carried out by spin coating at 3000 rpm for 20 s. The wet films were pre-annealed at 350 °C for 5 min and, followed by an annealing at 550 °C in air for 30 min. The above procedures were repeated several times to obtain the desired thickness. The structure of poly-BFO films was confirmed by checking the x-ray diffraction data (XRD) (D8 Bruker). Their leakage current behavior was characterized by a Keithley 2410 meter. The optical properties were measured by UV-Vis (Shimadzu UV 2501). The magnetic hysteresis (M-H) loops were collected using a vibrating sample magnetometer (VSM) (Lake Shore 7410).

3. Results and Discussions

Figure 1 shows the XRD spectra of the pure and Mn-doped BFO thin films grown on ITO/Glass substrates. The pure BFO film exhibits a polycrystalline perovskite structure with rhombohedral R3c symmetry which is in good agreement with literature results (i.e. JCPDS#20-0169) (Huang et al., 2009; Singh et al., 2006). The (104) and (110) diffraction peaks in the vicinity of $2\theta = 33.7^\circ$ are clearly separated in the pure BFO film, but the two peaks are shifted and overlapped to a single broad peak in the Mn-doped BFO films. This result implies that the rhombohedral distortion is reduced toward the tetragonal structure (P4mm) with increasing Mn concentration. Noted that the (012) diffraction peak is the strongest in the pure BFO film, but the (110) diffraction peak is the strongest one in the Mn-doped BFO film, which indicates Mn doping induced a different grain orientation growth in the BFO films. It is believed that this structural distortion and different grain orientation will be essential to the electric and magnetic property enhancement.

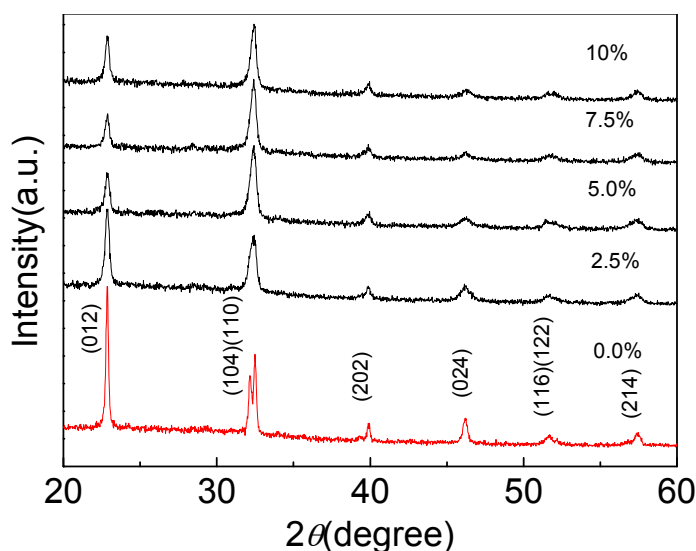


Figure 1. X-ray diffraction pattern of Mn-doped BiFeO₃

It is well known that the main disadvantage of the BFO film is its large leakage current which limits its applications in the field of micro-devices. Many efforts have been made to solve the problem. The site-engineering technique is thought to be a very effective ways to improve the electric properties of BFO film. The leakage current density of the Mn-doped BFO film was measured as a function of voltage as shown in Figure 2. It can be seen that Mn doping can effectively reduce the leakage current density of BFO thin film capacitor in the electric field region of 0~100 kV/cm. Pure and 10% Mn doped BFO films exhibit a larger

leakage current density than the samples with Mn 2.5%, 5.0% and 7.5% concentrations. These results imply that a small amount of Mn doping is a very effective ways to reduce the leakage current, but excess Mn doping leads to an increase in leakage current. The mechanisms responsible for the reduction of the leakage current in the Mn-doped BFO thin films concern the fact that Mn element can neutralize the donor action of the oxygen vacancies because the acceptor-type dopants can prevent the reduction of Fe^{3+} to Fe^{2+} . The Mn can compensate for the charges generated from the oxygen vacancies with the correct amount of charge balance to lower the leakage current (Kang et al., 2005). The leakage current behaviors are in good agreement with observations for the resistivity of the thin films as shown in Fig 3. It is shown that the resistivity increase with Mn amount increase in the Mn-doped (2.5%, 5.0% and 7.5%) thin films. However, it is also noticed that when Mn concentration reaches 10%, a lower resistivity are obtained. This result might be caused by the increase of free carrier density derived from the valence fluctuations of Mn ions under high Mn concentration ($\geq 10\%$) conditions (Kawae et al., 2009). The similar phenomena also can be observed in Figures 4 and 5.

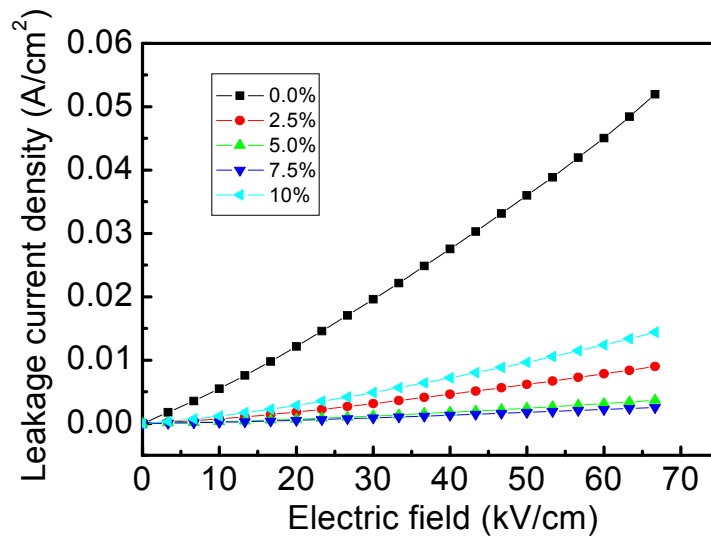


Figure 2. Variation of leakage current densities as a function of electric field of all samples

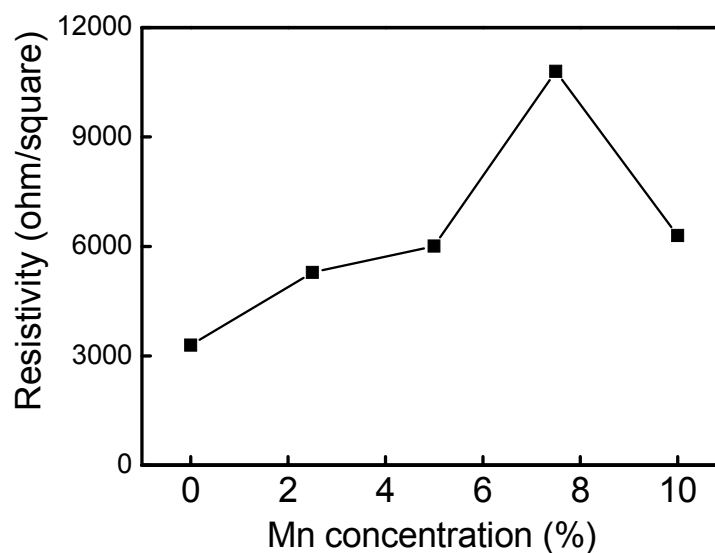


Figure 3. Resistivity of the samples as a function of Mn concentration

Figure 4 shows the M-H curves of the pure and Mn-doped BiFeO₃ thin films. According to Figure 4, all of the thin films show a saturated weak ferromagnetic hysteresis loops at room temperature. The saturated magnetization (M_s) of the pure and Mn 2.5%, Mn 5.0% and Mn 7.5% films is 39.4 emu/cm³, 89.0 emu/cm³, 96.2 emu/cm³, 110.1 emu/cm³, respectively. Compared with the pure BFO film, the saturated magnetization of BFO film with 2.5% Mn is improved evidently and then increases slightly with increasing Mn concentration. We thought two reasons might be responsible for the increases of the magnetization of the thin films. One could be that Mn atoms destroy the spin cycloid ordering originated from the Fe³⁺ and Fe²⁺, and then improve the magnetization value by decreasing Fe²⁺ influence on canting of Fe³⁺ spins in the unit cell. The other reason could be due to Jahn-Teller effect induced by structural distortion of the thin films which influences cation interactions and possibly gives rise to partial spin rearrangement. As Mn content is furtherly increased up to 10%, the saturated magnetization decrease. The reduced magnetization may be attributed to disturbing of valence change of part of Mn ions under high Mn concentration which may weaken the double exchange interactions from Fe³⁺-O-Mn²⁺.

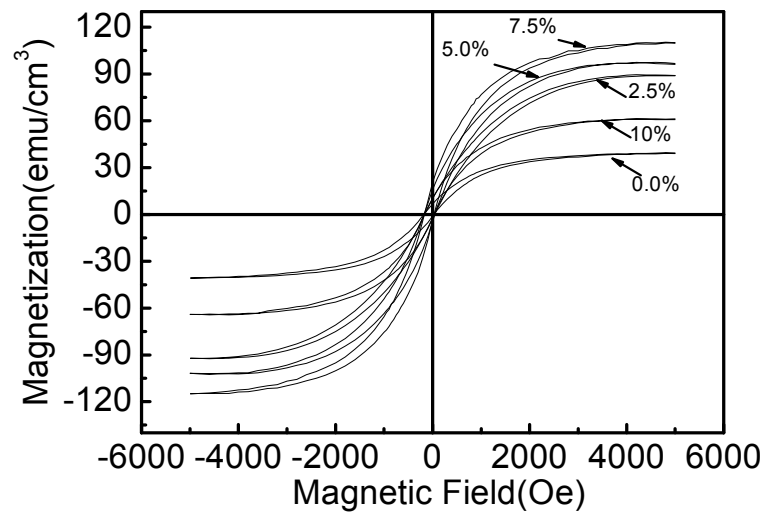


Figure 4. M-H curves of Mn-doped BiFeO₃ films

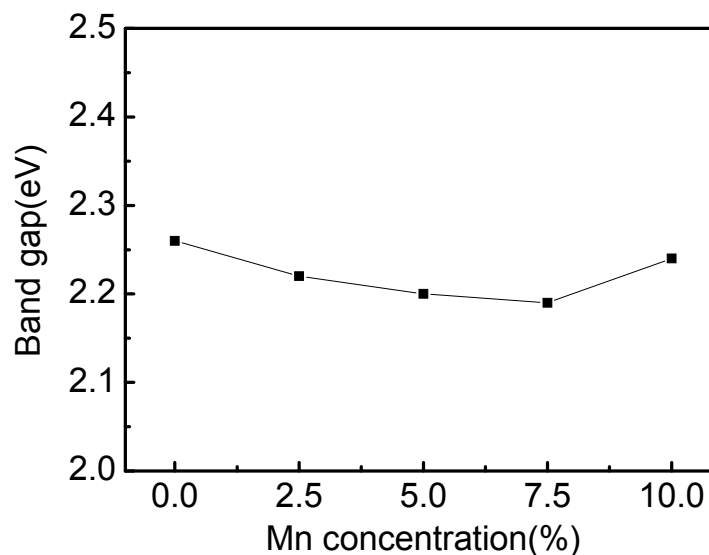


Figure 5. Band gap as a function of Mn concentration in BFO film

It has been known for several years that BFO film is an alternate choice for conventional semiconductor based photovoltaic devices because of their anomalous open-circuit voltage, in some cases >104 V, that were produced

when ferroelectrics are subject to illumination (Zang et al., 2011). However, its large band gap (typically ~2.7 eV) which limit the utilization of the materials for device applications. In this part, we studied further the effects of Mn atom on band gap of the BFO film grown on ITO/Glass substrates.

The optical energy band gap E_g for different samples was calculated by classical Tauc relation as given below (Singh et al., 2006):

$$\alpha hv = A(hv - E_g)^n \quad (1)$$

Where A is a constant, hv is the photon energy, E_g is the energy band gap, and α is absorption coefficient.

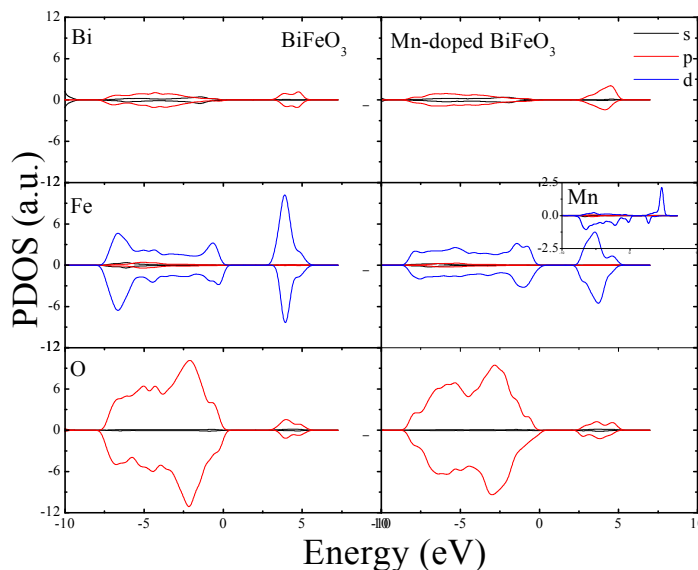


Figure 6. Partial density of states (PDOS) of pure BFO and Mn-doped BFO thin films

The plots of band gap versus Mn content for the thin films are shown in Figure 5. It can be found that the direct band gap decreases slightly with Mn content increase. The values of band gap are 2.26 eV, 2.22 eV, 2.20 eV and 2.19 eV for Mn-doped BFO thin films with Mn = 0, 2.5%, 5.0%, and 7.5%, respectively. First principles calculation shows that the Mn doping reduces the total enthalpy of BFO crystal structure from -13935.73 eV to -13737.89 eV and then influences the density of states (DOS) of the BFO film, as shown in Figure 6. Based on the PDOS results, Mn 3d⁵ orbit firstly is polarized over a range of 0-5 eV, and then degenerated with valence band of Fe 3d⁶ states which induce Fe energy levels shift to Fermi level. On the other hand, Mn 3d⁵ orbit provides the energy levels at 0-2.5 eV that degenerates Bi and O energy levels. Thus, the total band gap of the BFO film is reduced about 0.01 eV/lattice. The decreases of band gap of the BFO thin film is beneficial to transition of electrons from valence band to conductive band and then improve photoelectric conversion efficiency of the thin film solar cell.

4. Conclusions

In summary, the pure BiFeO₃ and Mn-doped BiFeO₃ thin films have been successfully deposited on the ITO/Glass substrates using Sol-gel technique. X-ray diffraction analysis revealed that the crystal structure and space group of the pure BFO film was rhombohedral with space group R3c symmetry and the Mn-doped BFO film was tetragonal crystal structure. Mn substitution increased the resistivity and then improved the leakage current characteristic of the BFO film by inhibiting oxygen vacancies. The saturated magnetization of Mn-doped BFO films were higher than that in the pure BFO film at a magnetic field of 6kOe at room temperature, and thus a saturated hysteresis loops in M-H characteristics are observed in these films. The saturated magnetization of Mn-substituted films increased slightly with increasing Mn concentration in the BFO film. Optical band gap varied slightly from 2.19 eV to 2.26 eV with increasing Mn concentration.

Acknowledgements

This work was financially supported by Youth Science Foundation of Xinjiang Uygur Autonomous Region of

China (2011211B49), the One Hundred Talents Project Foundation Program (1029271301), the West Light Foundation of The Chinese Academy of Sciences (Y12S311301, RCPY201206, XBBS201025), the science and technology Program of Urumqi (K121410007) and Fundamental Science on Nuclear Waste and Environmental Security Laboratory (12zxnp05).

References

- Huang, J. Z., Wang, Y., Lin, Y., Li, M., & Nan, C. W. (2009). Effect of Mn doping on electric and magnetic properties of BiFeO₃ thin films by chemical solution deposition. *Journal of Applied Physics*, 106(6), 063911-063915. <http://dx.doi.org/10.1063/1.3225559>
- Kang, K. T., Lim, M. H., Kim, H. G., Choi, Y., Tuller, H. L., Kim, I. D., & Hong, J. M. (2005). Mn-doped Ba_{0.6}Sr_{0.4}TiO₃ high-K gate dielectrics for low voltage organic transistor on polymer substrate. *Applied Physics Letters*, 87(24), 242908-242911. <http://dx.doi.org/10.1063/1.2139838>
- Kawae, T., Terauchi, Y., Tsuda, H., Kumeda, M., & Morimoto, A. (2009). Improved leakage and ferroelectric properties of Mn and Ti codoped BiFeO₃ thin films. *Applied Physics Letters*, 94(11), 112904-112907. <http://dx.doi.org/10.1063/1.3098408>
- Kumar, M. M., Palkar, V. R., Srinivas, K., & Suryanarayana, S. V. (2000). Ferroelectricity in a pure BiFeO₃ ceramic. *Applied Physics Letters*, 76(19), 2764-2766. <http://dx.doi.org/10.1063/1.126468>
- Kumar, M. M., Srinivas, A., & Suryanarayana, S. V. (2000). Structure property relations in BiFeO₃/BaTiO₃ solid solutions. *Journal of Applied Physics*, 87(2), 855-862. <http://dx.doi.org/10.1063/1.371953>
- Macchesn.Jb, Jetzt, J. J., Potter, J. F., Williams, H. J., & Sherwood, R. C. (1966). Electrical and Magnetic Properties of System SrFeO₃-BiFeO₃. *Journal of the American Ceramic Society*, 49(12), 644-647. <http://dx.doi.org/10.1111/j.1151-2916.1966.tb13191.x>
- Neaton, J. B., Ederer, C., Waghmare, U. V., Spaldin, N. A., & Rabe, K. M. (2005). First-principles study of spontaneous polarization in multiferroic BiFeO₃. *Physical Review B*, 71(1), 1-9. <http://dx.doi.org/10.1103/PhysRevB.71.014113>
- Singh, S. K., Ishiwara, H., & Maruyama, K. (2006). Room temperature ferroelectric properties of Mn-substituted BiFeO₃ thin films deposited on Pt electrodes using chemical solution deposition. *Applied Physics Letters*, 88(26), 262908-262911. <http://dx.doi.org/10.1063/1.2218819>
- Uchida, H., Ueno, R., Funakubo, H., & Koda, S. (2006). Crystal structure and ferroelectric properties of rare-earth substituted BiFeO₃ thin films. *Journal of Applied Physics*, 100(1), 014106-014109. <http://dx.doi.org/10.1063/1.2210167>
- Wang, J., Neaton, J. B., Zheng, H., Nagarajan, V., Ogale, S. B., Liu, B., ... Ramesh, R. (2003). Epitaxial BiFeO₃ multiferroic thin film heterostructures. *Science*, 299(5613), 1719-1722. <http://dx.doi.org/10.1126/science.1080615>
- Wei, J., Haumont, R., Jarrier, R., Berhtet, P., & Dkhil, B. (2010). Nonmagnetic Fe-site doping of BiFeO₃ multiferroic ceramics. *Applied Physics Letters*, 96(10), 102509-102512. <http://dx.doi.org/10.1063/1.3327885>
- Wu, J. G., Wang, J., Xiao, D. Q., & Zhu, J. G. (2011). Impedance spectroscopy of bilayered bismuth ferrite thin films. *Journal of Applied Physics*, 110(6), 064104-064107. <http://dx.doi.org/10.1063/1.3636390>
- Yun, K. Y., Noda, M., & Okuyama, M. (2003). Prominent ferroelectricity of BiFeO₃ thin films prepared by pulsed-laser deposition. *Applied Physics Letters*, 83(19), 3981-3983. <http://dx.doi.org/10.1063/1.1626267>
- Yun, K. Y., Noda, M., Okuyama, M., Saeki, H., Tabata, H., & Saito, K. (2004). Structural and multiferroic properties of BiFeO₃ thin films at room temperature. *Journal of Applied Physics*, 96(6), 3399-3403. <http://dx.doi.org/10.1063/1.1775045>
- Zang, Y. Y., Xie, D., Wu, X., Chen, Y., Lin, Y. X., Li, M. H., ... Plant, D. (2011). Enhanced photovoltaic properties in graphene/polycrystalline BiFeO₃/Pt heterojunction structure. *Applied Physics Letters*, 99(13), 132904-132907. <http://dx.doi.org/10.1063/1.3644134>
- Zeches, R. J., Rossell, M. D., Zhang, J. X., Hatt, A. J., He, Q., Yang, C. H., ... Ramesh, R. (2009). A Strain-Driven Morphotropic Phase Boundary in BiFeO₃. *Science*, 326(5955), 977-980. <http://dx.doi.org/10.1126/science.1177046>
- Zhang, Q., Kim, C. H., Jang, Y. H., Hwang, H. J., & Cho, J. H. (2010). Multiferroic properties and surface

potential behaviors in cobalt-doped BiFeO₃ film. *Applied Physics Letters*, 96(15), 152901-152903.
<http://dx.doi.org/10.1063/1.3391667>

Copyrights

Copyright for this article is retained by the author(s), with first publication rights granted to the journal.

This is an open-access article distributed under the terms and conditions of the Creative Commons Attribution license (<http://creativecommons.org/licenses/by/3.0/>).